energies

MDPI

Article

Performance Evaluation of Burkina Faso's 33 MW Largest Grid-Connected PV Power Plant

Sami Florent Palm [1,2,*], Lamkharbach Youssef [2], Sebastian Waita [1], Thomas Nyachoti Nyangonda [1], Khalid Radouane [2] and Ahmed Chebak [2]

[1] Condensed Matter Research Group, Department of Physics, University of Nairobi, Nairobi P.O. Box 30197-00100, Kenya; swaita@uonbi.ac.ke (S.W.); nyangondat@uonbi.ac.ke (T.N.N.)
[2] Green Tech Institute, Mohammed VI Polytechnic University, Ben Guerir 43150, Morocco; youssef.lamkharbach@um6p.ma (L.Y.); khalid.radouane@um6p.ma (K.R.); ahmed.chebak@um6p.ma (A.C.)
* Correspondence: palm.sami7@gmail.com or palm@students.uonbi.ac.ke

Abstract: This study conducted an in-depth analysis of the performance of the largest Grid-Connected Solar Photovoltaic System in Burkina Faso from 2019 to 2021. The research utilized measured data and simulated the plant's performance using the PVGIS database. The results revealed that the months with high solar radiation were the most energy-productive, indicating a direct correlation between solar irradiance and energy generation. During the rainy season (July and August), the PV plant exhibited the highest conversion efficiency. Conversely, the hot season (March and April) was associated with the lowest conversion efficiencies, with module temperatures reaching approximately 47 °C. Efficiency decreased from 12.29% in 2019 to 12.10% in 2021. The system's performance ratio ranged from 80.73% in 2019 to 79.36% in 2021, while the capacity factor varied from 19.89% in 2019 to 19.33% in 2021. The final yield, measured in hours per day, was 4.89 h/d in 2019, 4.61 h/d in 2020, and 4.92 h/d in 2021. These findings highlight the deterioration in the performance of the Zagtouli PV plant over time. The study emphasizes the utility of using PVGIS-SARAH2 to forecast solar radiation and estimate energy output in PV systems. A semi-automatic cleaning system is used to clean the modules. This cleaning mechanism is inefficient because it is inconsistent. To increase the PV plant's effectiveness, improved cleaning systems with more advanced mechanisms are required. This research, the first of its kind on the largest PV power plant connected to Burkina Faso's national grid, serves as a valuable model for other power plants currently under construction or in the planning stages.

Keywords: performance analysis; grid-connected PV system; temperature effect; conversion efficiency

Citation: Palm, S.F.; Youssef, L.; Waita, S.; Nyangonda, T.N.; Radouane, K.; Chebak, A. Performance Evaluation of Burkina Faso's 33 MW Largest Grid-Connected PV Power Plant. *Energies* **2023**, *16*, 6177. https://doi.org/10.3390/en16176177

Academic Editor: Surender Reddy Salkuti

Received: 5 June 2023
Revised: 8 July 2023
Accepted: 21 July 2023
Published: 25 August 2023

1. Introduction

Fossil fuel-based energy is a major contributor, accounting for over 75% of global greenhouse gas emissions, thus significantly contributing to global climate change [1]. To address this critical issue, the development of renewable energy sources like wind and solar power, along with innovative approaches such as the storage of excess electricity using Molten Salt technology, holds great potential for mitigating this problem [2].

Despite the prevailing global pandemic, the photovoltaic (PV) market has exhibited consistent growth, with projections indicating a global PV market size of 175 GW by 2021 [3]. Throughout 2021, the cumulative capacity of newly commissioned PV plants worldwide amounted to 945.7 MW, with approximately 70% of this capacity installed within the preceding five years [3]. These statistics underscore the mainstream adoption of solar PV as a prominent source of electricity and its pivotal role in facilitating the transition towards cleaner energy worldwide. Solar PV systems have emerged as indispensable tools for decarbonizing the electricity sector, showcasing significant advancements over the past decade and presenting immense prospects for the year 2050. Africa's installed solar PV capacity represented a modest 1.35% of the global installed capacity in 2020, emphasizing

the need for substantial efforts to increase this figure [4]. According to the 2020 report from Burkina Faso's National Electricity Company (SONABEL), the national electricity generation fleet's nominal installed capacity at the end of 2020 was 366.05 MW. The distribution of this capacity was as follows: 299.95 MW from fuel thermal generation, 32 MW from hydroelectric power, and 34.1 MW from solar PV. The report highlights the dominance of thermal power generation using fossil fuels and the persistent shortfall in meeting growing electricity demand. More than half of the electricity consumed in Burkina Faso is imported from neighboring countries like Cote d'Ivoire and Ghana. To achieve sustainable development goals, the Burkina Faso government has made strategic investments in deploying large-scale solar PV systems [5]. Notable solar PV plants, including the 33 MW Zagtouli plant, the 1.1 MW Ziga plant, and the 30 MW Nagrengo plant, have been successfully commissioned. In 2020, the combined electricity generation from the Zagtouli and Ziga plants will account for nearly 3% of the country's total electricity production. Figures 1 and 2, presented below, illustrate the annual installed solar PV capacity worldwide and in Burkina Faso, respectively, from 2011 to 2020 [4].

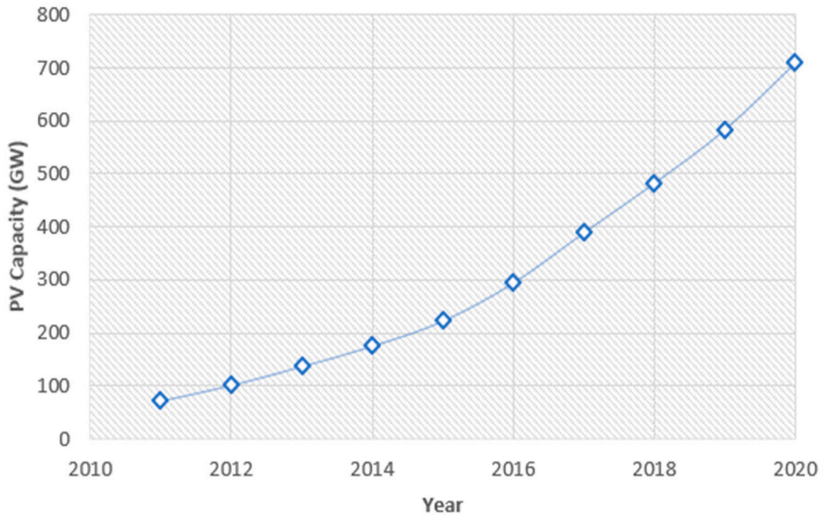

Figure 1. Annual Solar PV Capacity installed in the world.

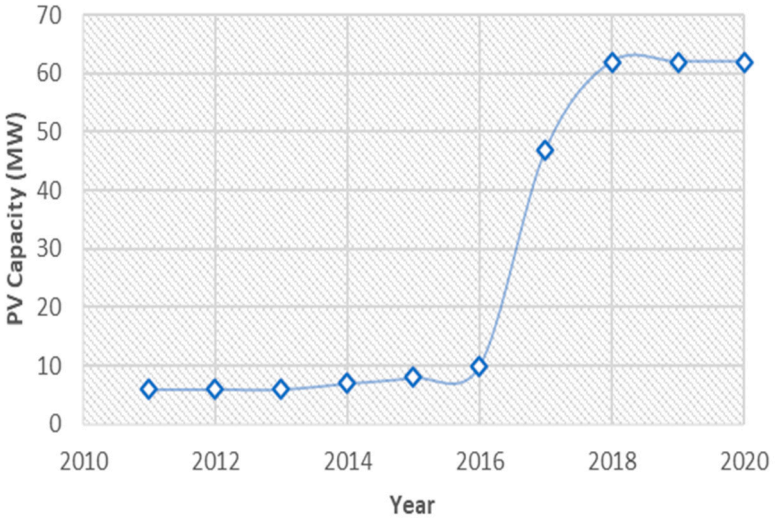

Figure 2. Annual Solar PV Capacity Installed in Burkina Faso.

Evaluating the performance of photovoltaic (PV) systems in different locations has been a subject of research, considering the influence of various factors, including environmental conditions. Attari et al. [6] used real performance parameters to monitor a PV

system in Tangier for one year. The annual performance ratio and the capacity factor of 79% and 14.83%, respectively, showed that the PV system was operating effectively. A PV system's performance ratio and capacity factor in northeastern Brazil, as determined by De Lima et al. [7], were 82.9% and 19.2%, respectively. Venkatesh et al. [8] used SCADA data from April 2018 to March 2019 to investigate the performance of a 50 MW PV power plant in southern India. The results obtained for the annual average performance ratio and capacity utilization factor were 79.94% and 24.65%, respectively. Ouedraogo et al. [9] used data recorded by the off-grid PV system installed at the Charle de Gaulle pediatric hospital in Ouagadougou to examine its efficiency. The findings indicated that May was the most productive month for this PV system, but due to the ongoing lack of energy from the national grid during this month, the PV system's storage capacity needs to be increased to ensure a steady supply of electricity. From 2012 to 2019, Johannes et al. [10] studied the performance of 32,744 roof-top PV systems in six European countries (the Netherlands, Belgium, Luxembourg, Germany, France, and Italy). The results revealed that the average performance ratio of each system was around 73%. Mihor et al. [11] conducted an evaluation study on a 194.93 kWp solar park in Ruse, Bulgaria, where the average capacity factor and performance ratio values were 11.54% and 70.44%, respectively, which are extremely low when compared to previous locations. Bouacha et al. [12] analyzed the performance of the first grid-connected PV system in Algeria using monitoring data. The study revealed unusual performance ratios, suggesting the need for a thorough investigation to identify and address the underlying issues. Theoretically, the approaches used in the aforementioned studies are not sufficient to characterize the performance analysis of PV systems because of some missing data. The authors in [13] conducted the first database performance analysis of the time series performance of PV systems installed in Europe, allowing them to assess the quality of large amounts of data to conduct a more accurate study of PV system performance. Thus, comparative studies between the measured approach and the simulated approach are necessary. Enrique Fuster et al. [14] assessed the performance of a grid-connected PV plant in central Spain after 12 years of operation, first using on-site data for 2020 and then two other modeling approaches, namely the physical model and the statistical model based on the random forest algorithm. The random forest approach, which used only ambient temperature and solar radiation as inputs, produced good results when the metric parameters were considered. Maria et al. [15] also used various statistical methods to evaluate the degradation rate of a large-scale grid-connected PV plant in India. The results have shown that the Classical Seasonal Decomposition (CSD) and the Seasonal and Trend decomposition using Loess (STL) are better than the Linear Least-Squares regression (LLS) and Holt-Winter seasonal model (HW). The researchers in [16–22] have mostly used actual on-site measurements and software such as PV GIS, PV SYST, HELİOSCOPE, HOMER, SAM, RETSREEN, and MATLAB to carry out comparative studies of solar PV systems. These studies show that the performance results simulated by these software packages are close to the measured performance results. However, some software packages give more accurate results than others. In Malaysia, Saleheen et al. [23] concentrated on calculating target performance using a simple model and measurements. The preceding study demonstrated the target-oriented model's dependability.

However, limited research has been conducted in Burkina Faso on the evaluation of large-scale PV systems through a comparison of measured and simulated performance. This study aims to evaluate the performance of the Zagtouli Grid-Connected Solar PV System (ZGCSPS) using both measured data and the PVGIS database, particularly PVGIS-SARAH2 [24]. In fact, this study presents a comprehensive assessment of the performance of a PV plant in Burkina Faso, utilizing real-time data acquired from the Supervisory Control and Data Acquisition (SCADA) system. The analysis includes various performance metrics such as the performance ratio, capacity factor, annual yields, loss factors, energy efficiency, module temperature, and inverter efficiency. The obtained performance results are compared with the simulated model from the PVGIS database. Furthermore, the study investigates the impact of temperature on PV plant performance and examines the annual

degradation rate over a three-year operational period. The validity of the findings is further enhanced through a comparative analysis with other PV plants worldwide, taking into consideration site conditions, installed capacity, final yield, and performance ratio (PR).

The structure of the paper is as follows: Sections 1 and 2 provide an introduction and outline the general specifications of the ZGCPVS. Section 3 presents an explanation of the experimental approach and the method employed for performance evaluation. Section 4 focuses on a comprehensive analysis of the performance data and presents the findings. Additionally, Section 5 discusses the socio-economic impacts of the ZGCPVS. Finally, the conclusions section summarizes the key findings and implications of this research.

2. The Zagtouli Grid-Connected PV System (ZGCPVS)

2.1. Geographical Location

The ZGCPVS, with a capacity of 33 MW, is situated near National Road Number 1 (N1) in Ouagadougou, the capital of Burkina Faso. Its precise geographical coordinates are approximately longitude 12.30702° and latitude −1.63548°. The specific location of the Zagtouli PV plant can be seen in Figure 3.

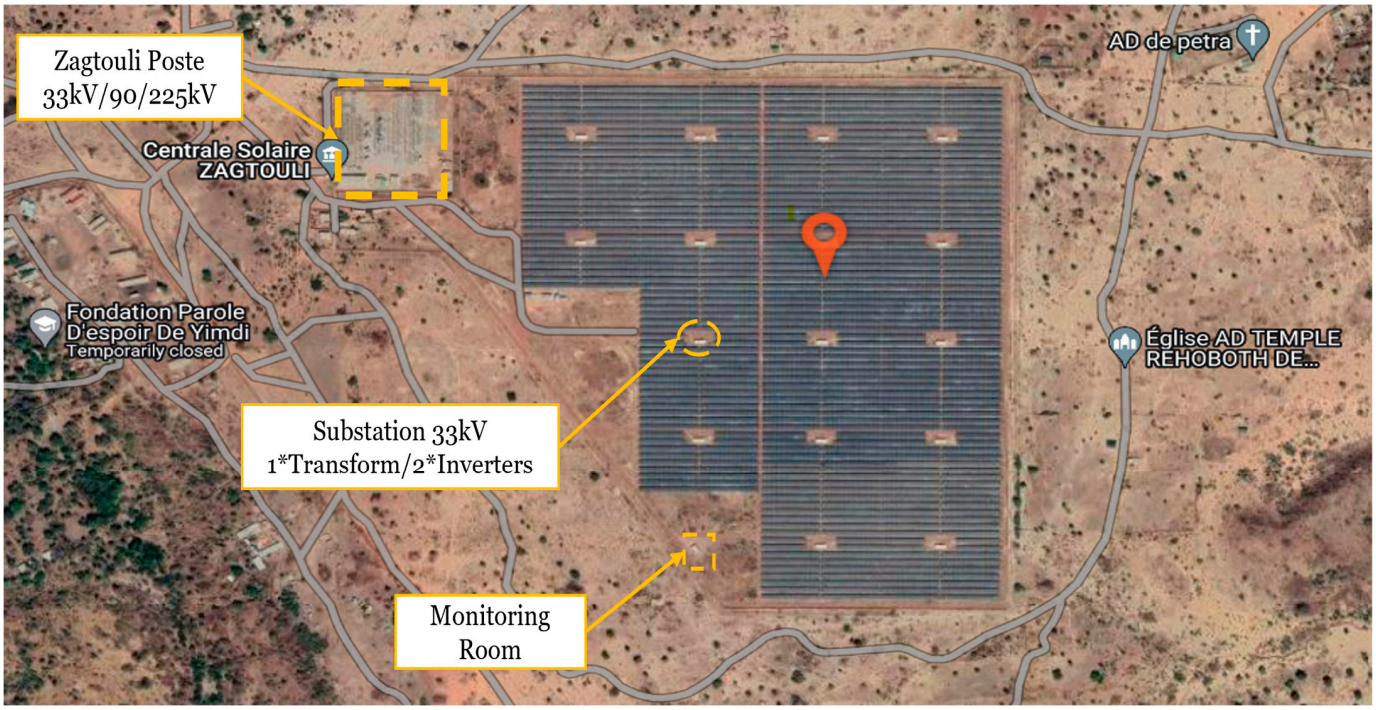

Figure 3. Zagtouli PV plant location. source: google Maps.

2.2. Characteristics

The ZGCPVS installed power is 33.696 MWp, arranged in 5400 strings of 24 modules of 260 Wp polycrystalline Silicon (p-si) type in series and connected to 32 inverters of 1.1 MW operating 2 by 2 in master-slave mode, with each pair of inverters associated with a transformer of 2330 kVA. The energy output from the 16 subsystems [Figure 4] is fed into the main transformer (33 kV/90/225 kV, 50 Hz) for grid interconnection. The specifications of the modules and inverters installed in the plant and used in this study are shown in Tables 1 and 2.

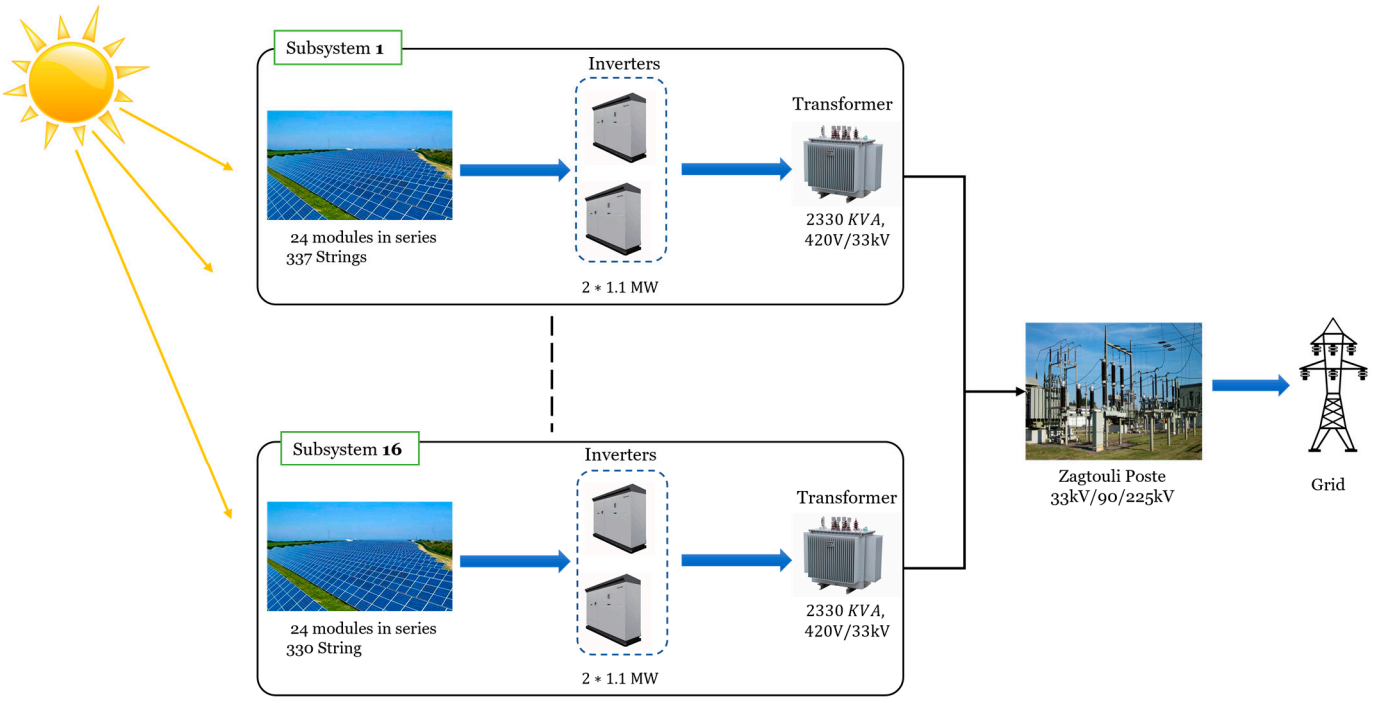

Figure 4. Zagtouli PV Plant Structure.

Table 1. Sunmodule Plus SW 260 Poly characteristics at STC.

PV Panel Parameters	Parameters	Values
nominal power	Pmax	260 W
Open circuit voltage	Voc	37.6 V
Maximum power voltage	Vmp	30.8 V
Short circuit current	Isc	9.06 A
Maximum power current	Imp	8.54 A
Efficiency	η	15.9%
Temperature coefficient of Isc	Ki	0.051%/K
Temperature coefficient of Voc	Kv	−0.31%/K
Temperature coefficient of Pmax	Kp	−0.41%/K
Maximum system voltage	...	1000 V
Operating temperature	...	(−40 to +85) °C
NOCT	...	46 °C

Table 2. Ingecon Sun 1165TL B420 Inverter characteristics.

Inverter Parameters	Values
Maximum PV input voltage	1050 V
Maximum PV input current	2000 A
MPPT Voltage range	(610–820) V
Maximum AC output power	1165 W
Nominal AC operating voltage	420 V
Efficiency	98%
Temperature range	(−20 to +55) °C

2.3. Solar PV Modules Cleaning System

The accumulation of dirt and debris on solar PV modules, known as "soiling" can have a detrimental effect on the efficiency of the ZGCPVS. Studies have shown that the degradation in efficiency can range up to 4% depending on environmental conditions and the type of solar modules used [25]. In particularly harsh environments with high levels

of dust and strong winds, the output of a solar PV system that has not been cleaned for a month can drop by up to 50% [26]. There are three main methods for cleaning solar PV modules: manual, semi-automatic, and fully automatic [25]. The manual method requires a significant amount of labor and is associated with lower investment costs for cleaning equipment. The semi-automatic method involves less manual labor and has a lower initial investment cost compared to the manual method. On the other hand, the fully automatic method utilizes robots and advanced sensors to optimize the cleaning process while ensuring the profitability of PV systems. However, the fully automatic method comes with a higher initial investment cost compared to the other two methods.

In the case of ZGCPVS, a semi-automatic cleaning system is employed, as shown in Figure 5. Cleaning campaigns are conducted from January to March and from November to December, as indicated in Table 3. These cleaning campaigns rely heavily on fossil fuel, which has negative environmental impacts and increases the operation and maintenance costs of the ZGCSPS. Additionally, the intermittent nature of these cleaning campaigns reduces the energy profitability of the plant.

Figure 5. Zagtouli PV Plant semi-automatic cleaning System.

Table 3. Report on the cleaning of Zagtouli PV modules for the year 2022.

	Campaign 1	**Campaign 2**	**Campaign 3**	**Campaign 4**	**Campaign 5**	**Total Annual**
Period	From 01/04/2022 to 01/17/2022	From 01/30/2022 to 02/09/2022	From 02/10/2022 to 03/17/2022	From 11/02/2022 to 11/28/2022	From 11/29/2022 to 12/31/2022	
Water volume used (m^3)	94	126	79	144	177	620
Diesel quantity for the tractor (m^3)	0.320	0.280	0.440	0.620	0.820	2.480
fuel volume for the motor pump (m^3)	0.0045	0.0045	0.0055	0.023	0.025	0.0625
tractor running time (hour)	55	76	78	117	136	462
hydraulic oil for the tractor (m^3)	...	...	0.004	0	0.001	0.005
number of working days	17	13	19	19	10	78

Furthermore, the data presented in Table 3 indicates that the PV modules were cleaned on only 78 out of the 365 days in 2022. The low cleaning rate can be attributed to challenges in mobilizing financial resources to hire staff, procure fuel, and obtain cleaning accessories, as reported by the plant management. To improve profitability and reduce cleaning costs, it is crucial to explore optimization strategies for enhancing the cleanability of power plant modules.

One potential solution is the implementation of a more sophisticated cleaning method, such as a self-cleaning mechanism. This innovative approach offers several benefits, including reduced operating and maintenance costs, regulation of module temperature to prevent overheating, recycling of cleaning water, and even the recovery of rainwater [26]. By adopting such advanced cleaning techniques, the Zagtouli PV plant could significantly increase its output and improve its overall performance.

3. Materials and Method

3.1. Data Collection Processes

Data were recorded for three years: 2019, 2020, and 2021. There are four weather stations on the PV plant site. These stations have been placed in particular areas of the power plant: one at the top of the Supervisory Control and Data Acquisition (SCADA) building (Figure 6), and the others on the PV array site (Figure 7), which measure the ambient temperature, module temperature, wind speed, wind direction, relative humidity, irradiance (global and direct horizontal), and tilt angle of PV modules. These measurements are recorded every minute.

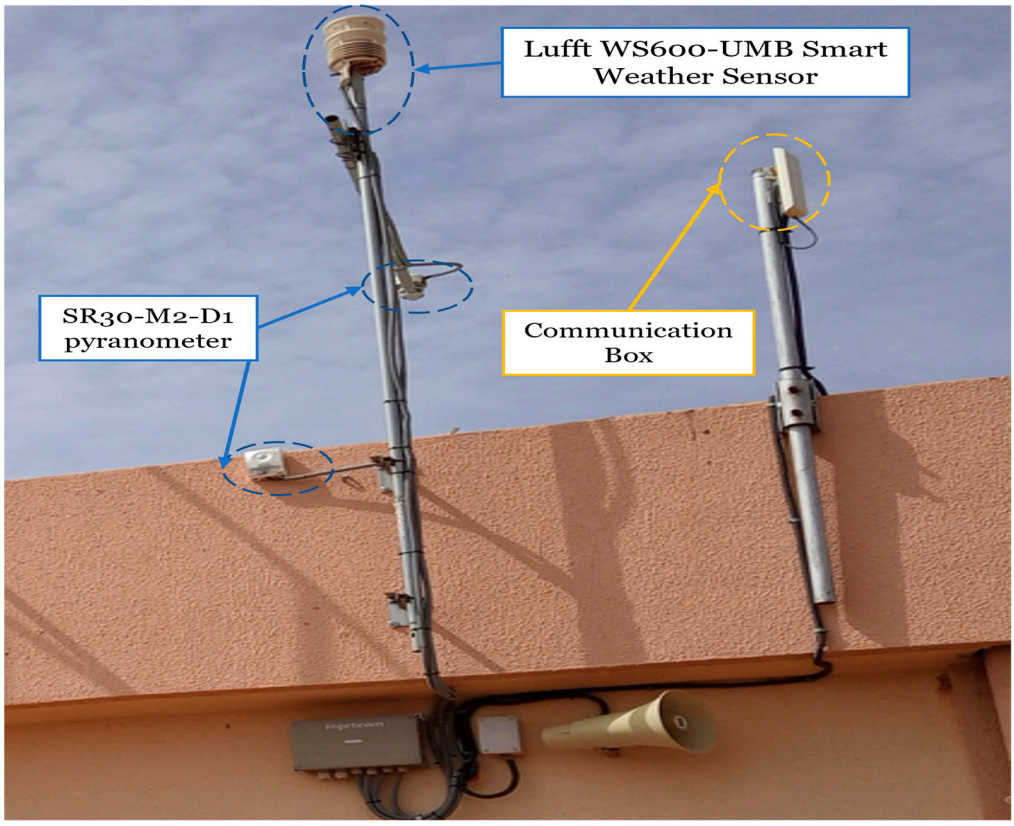

Figure 6. Weather Station on the top of the Monitoring room.

To measure the temperature of the modules, temperature sensors are installed on their backs. In the same area, both direct and alternating currents and voltages are recorded through other sensors in the PV plant. Table 4 below shows the characteristics of the different sensors used, while Figure 8 below gives an overview of the SCADA.

Figure 7. Weather Station in the PV array site.

Table 4. Characteristics of Sensors.

Parameter	Sensor	Measurement Range	Accuracy
Wind Speed	Lufft WS600-UMB Smart Weather Sensor	0–246.06 ft/s (0–75 m/s)	Wind Speed: ±0.3 m/s or ±3% (0–35 m/s) ± 5% (>35 m/s) RMS
Wind Direction	Lufft WS600-UMB Smart Weather Sensor	0–359.9°	<3° RMSE > 1.0 m/s
Ambient temperature	Lufft WS600-UMB Smart Weather Sensor	−50. . .60 °C	±0.2 °C (−20. . .50 °C), otherwise ±0.5 °C (>−30 °C)
Relative humidity	Lufft WS600-UMB Smart Weather Sensor	0. . .100% RH	±2% RH
GHI & DHI	SR30-M2-D1 pyranometer	285 to 3000 nm	<±3% ((0.35 to 1.5) × nm)
tilt sensor	SR30-M2-D1 pyranometer	0 to 90°	±1° (0 to 90°)

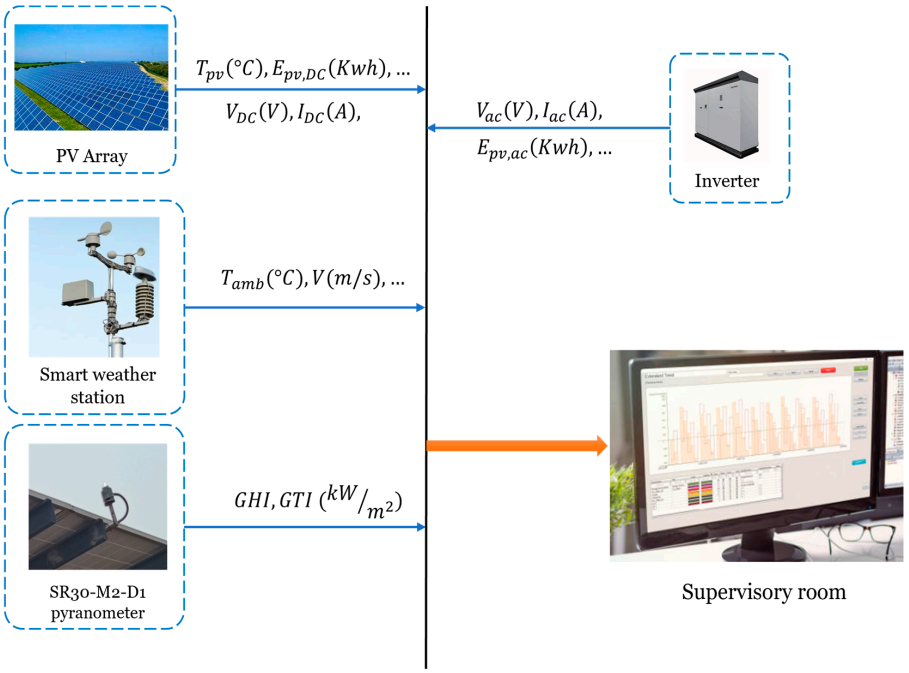

Figure 8. Diagram of the SCADA overview.

3.2. Quantitative Parameters

IEC Standard 61724 [27] specifies the method for quantitatively evaluating the performance of grid-connected PV systems.

3.2.1. PV Array Energy Production

The daily $E_{dc,d}$ and monthly, $E_{dc,m}$ DC energies are respectively given by [28]:

$$E_{dc,d} = \sum_{t=1}^{t=t_{rp}} V_{dc} \times I_{dc} \times T_r \quad (1)$$

$$E_{dc,m} = \sum_{d=1}^{N} E_{dc,d} \quad (2)$$

with T_r the time step, t_{rp} being the reporting period, and N being the number of days in a month that the PV plant is operational.

3.2.2. Energy Supplied into the Grid

Energy Supplied into the Grid represents the energy produced by the GCSPS across the inverter output terminals. $E_{ac,d}$, and $E_{ac,m}$ are respectively the total daily and total monthly AC energy output. Their respective expression is given by [28]:

$$E_{ac,d} = \sum_{t=1}^{t=t_{rp}} V_{ac} \times I_{ac} \times T_r \quad (3)$$

$$E_{ac,m} = \sum_{d=1}^{N} E_{ac,d} \quad (4)$$

3.2.3. Reference Yield (Y_R)

Reference Yield evaluates the sun's availability to produce solar energy at a specific location and time [29]. It is given by [15]:

$$Y_R = \frac{H}{G_{STC}} \text{ (h/day)} \quad (5)$$

3.2.4. Array Yield (Y_A)

Array Yield is known as the ratio of energy generated $E_{PV,DC}$ (kWh) to its rated power P_{nom} (kWp) under specific conditions [30,31]. In other words, it is the amount of time the system needs to run at its nominal power to generate the same amount of energy at the PV array's output [16]:

$$Y_A = \frac{E_{PV,DC}}{P_{nom}} \text{ (h/day)} \quad (6)$$

3.2.5. Final Yield (Y_F)

Final Yield is a parameter that determines how long the system has been operating at the nominal power P_{nom} (kWp), to generate the inverter's output energy, $E_{PV,AC}$ (kWh) [32]. It is given as:

$$Y_F = \frac{E_{PV,AC}}{P_{nom}} \text{ (h/day)} \quad (7)$$

Figure 9 below shows the details of the system's yields.

3.2.6. Performance Ratio (P_R)

The Performance Ratio denotes the proportion of usable energy at the output of the PV system after all losses. It also represents the real amount of energy generated by a solar PV system compared to the theoretical energy under the same irradiance condition, as given by [16,29,32]:

$$P_R = \frac{Y_F}{Y_R} \times 100 \text{ (\%)} \quad (8)$$

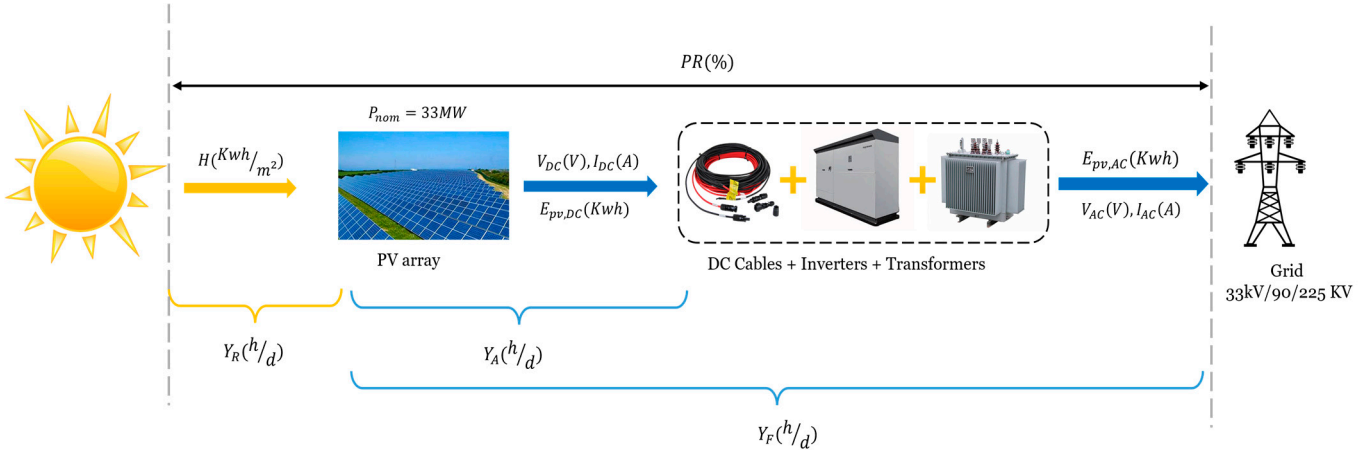

Figure 9. System yields overview.

3.2.7. Array Capture Losses (L_C)

Array Capture losses serve as a representation of the variation between the array yield and the reference yield and are given by [31]:

$$L_C = Y_R - Y_A \text{ (h/day)} \quad (9)$$

Loss of L_C grid capture indicates a problem with the PV system's DC component [33].

3.2.8. System Losses (L_S)

These losses result from the PV array's DC energy being converted into grid-compatible AC energy, as calculated by [30]:

$$L_S = Y_A - Y_F \text{ (h/day)} \quad (10)$$

DC cables, inverters, transformers, and other passive circuits are responsible for these losses [29]. Figure 10 below represents a diagram of the system losses.

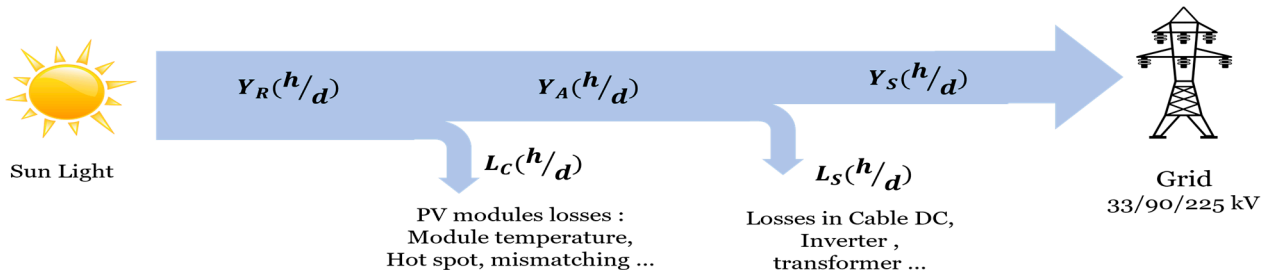

Figure 10. System losses diagram.

3.2.9. PV System Efficiency (η)

The proportion of energy produced to energy collected by the PV system is measured as system efficiency η and it can be calculated as [33–36]:

$$\eta = \frac{E_{PV,AC}}{H \times A} \times 100 \ (\%) \quad (11)$$

H (kWh/m^2) denotes the solar irradiation, and A (m^2) is the total PV array area.

3.2.10. Capacity Factor (CF)

This parameter refers to the ratio of a PV system's annual AC energy produced to the energy it should generate under standard conditions and is an important indicator for

assessing the system's ability to operate under actual environmental conditions to make the system's energy available [15]. It enables the evaluation of the efficiency of solar technology in a specific location. It is determined by [15,37]:

$$CF = \frac{Annual\ energy\ produced\ (\text{kWh})}{PV\ power\ rated\ (\text{kW}) \times 8760\ (\text{h})} \times 100\ (\%) \quad (12)$$

3.3. Qualitative Parameters

The energy quality index of a system is assessed using the exergy of the system [35]. This parameter is used in this study to compare the energy output of the Zagtouli PV plant.

3.3.1. Solar Radiation Exergy (b_s)

The exergy b_s (kWh) provided by incoming solar radiation is given by [35]:

$$b_s = \left[1 + \left(\frac{1}{3}\right)\left(\frac{T_a}{T_s}\right)^4 - \left(\frac{4}{3}\right)\left(\frac{T_a}{T_s}\right)\right] \times A \times H \quad (13)$$

T_a represents the ambient temperature (°C) and T_s the sun temperature (°C), with T_s = 5430 °C.

3.3.2. Exergy Efficiency (Γ)

Exergy Efficiency is the proportion of energy generated $E_{PV,AC}$ (kWh) to the solar radiation exergy b_s (kWh) that the PV array has captured. The exergy efficiency Γ (%) is expressed as follows [35]:

$$\Gamma = \frac{E_{PV,AC}}{b_s} \times 100\ (\%) \quad (14)$$

4. Results and Discussions

The real-time results of the (SCADA) System are compared and analyzed using the PVGIS-SARAH2 database. Measured in-plan solar irradiation is compared to simulated solar irradiation for the years 2019, 2020, and 2021 in Figure 11.

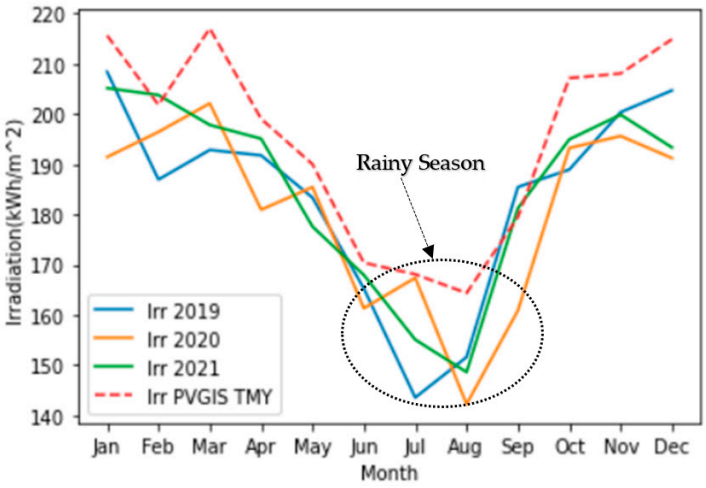

Figure 11. Comparison between measured and SARAH 2 monthly solar irradiation for the years 2019, 2020, and 2021.

A harmonious evolution of solar irradiation through its two approaches is observed, with significant solar radiation of up to 200 kWh/m^2, excluding the rainy season from June to September, where solar irradiation ranges between 140 kWh/m^2 and 180 kWh/m^2. Figure 12 clearly shows that the measured monthly irradiance values for 2019, 2020, and 2021 are

very close to the simulated values using the PVGIS-SARRAH2 database. The correlation coefficients for 2019, 2020, and 2021 are 0.907722, 0.91771586, and 0.9214544, respectively.

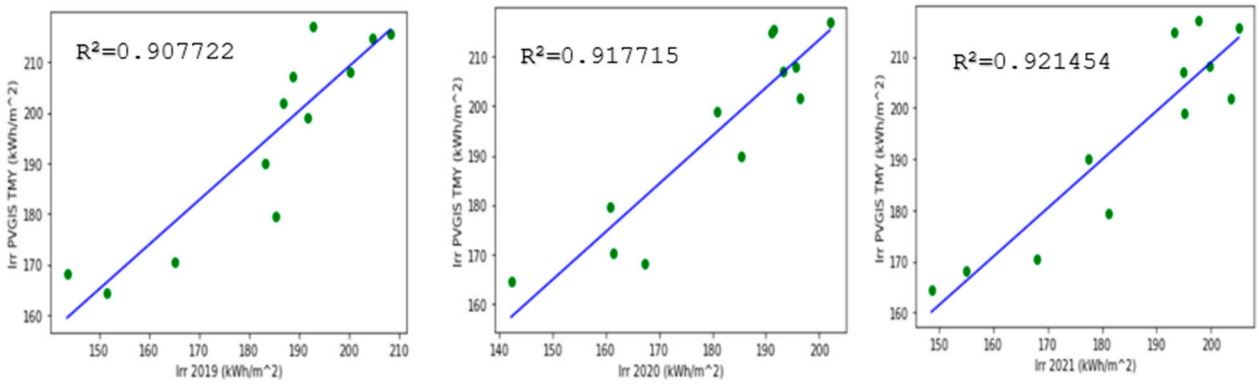

(**a**) (**b**) (**c**)

Figure 12. Correlation between measured irradiance for the years (**a**): 2019, (**b**): 2020, and (**c**): 2021 against irradiance from PVGIS-SARRAH.

The evolution of the measured ambient temperature (Ta) and the measured module temperature (Tm) for the years 2019, 2020, and 2021 is depicted in Figure 13. During the daily operating time of the PV system, i.e., from 6:00 to 18:00, Tm is constantly higher than Ta, with a maximum difference of about 25 °C. Also, Tm remains very high during the dry season (March to April), reaching up to 47 °C, and very low during the rainy season (June to September).

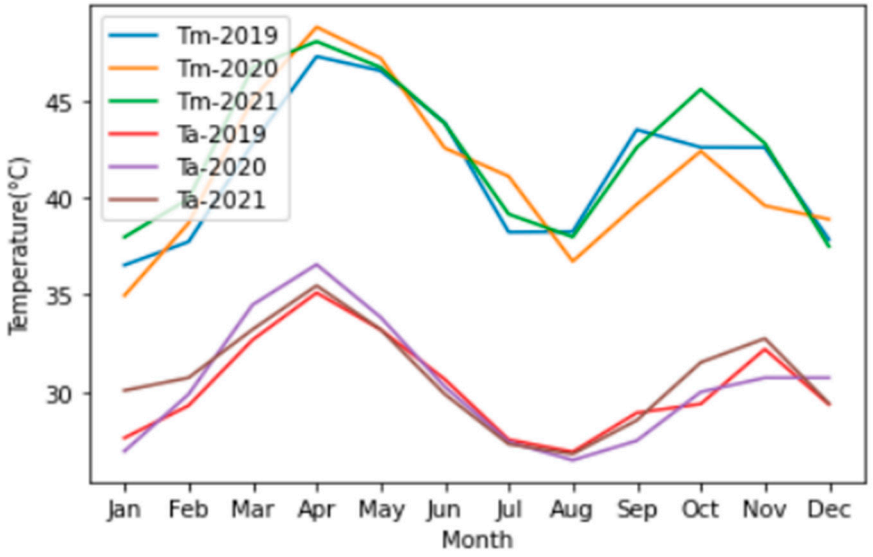

Figure 13. Monthly Evolution of ambient (Ta) and Module (Tm) Temperatures.

Figure 14 shows the monthly evolution of yields during the years 2019 and 2020. It is noticed that reference yield (Y_R) is always the highest, while array yield (Y_A) and final yield (Y_F) are lower and nearly equal, with array yield (Y_A) being marginally higher than final yield (Y_F) due to conversion losses, contact resistances, and cable resistances. During the rainy season (June, July, and August) and the hotter season (March, April, and May), the system yield is inadequate. However, the cold season (November, December, January, and February) is extremely beneficial to the system's operation.

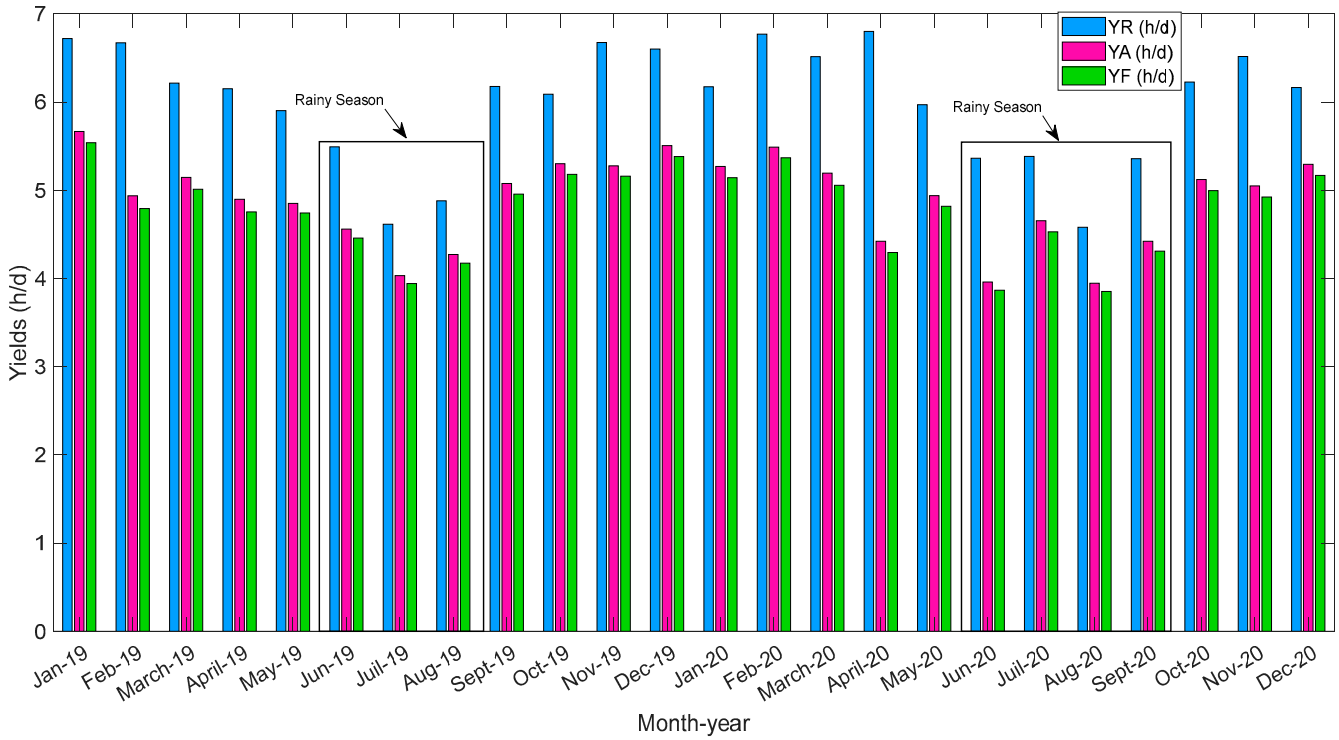

Figure 14. Monthly variation of daily Yields for the years 2019 and 2020.

Figure 15 depicts a strong relationship between solar irradiation and final yield.

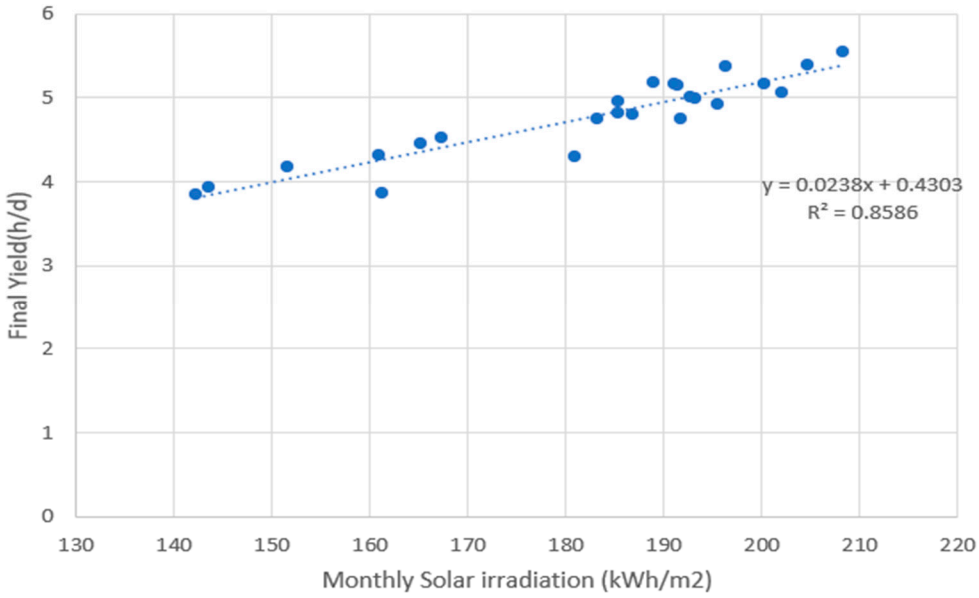

Figure 15. Correlation between final yield and solar irradiation.

Figure 16 shows the performance ratio and module temperature monthly evolution for the monitoring period. Optimum performance ratios are noticed in the wettest months (July, August, and September) and the seasons when module temperatures are at their lowest (November, December, January, and February). In 2019, 2020, and 2021, the performance ratios were 80.73%, 78.70%, and 79.36%, respectively. This result revealed a performance ratio degradation, with even more degradation in the year 2020 due to a module cleaning issue. The performance ratio is the portion of energy available after all system losses and

is impacted by several parameters (dust, module temperature, module type, inverter and cable efficiency, PV system condition, etc.).

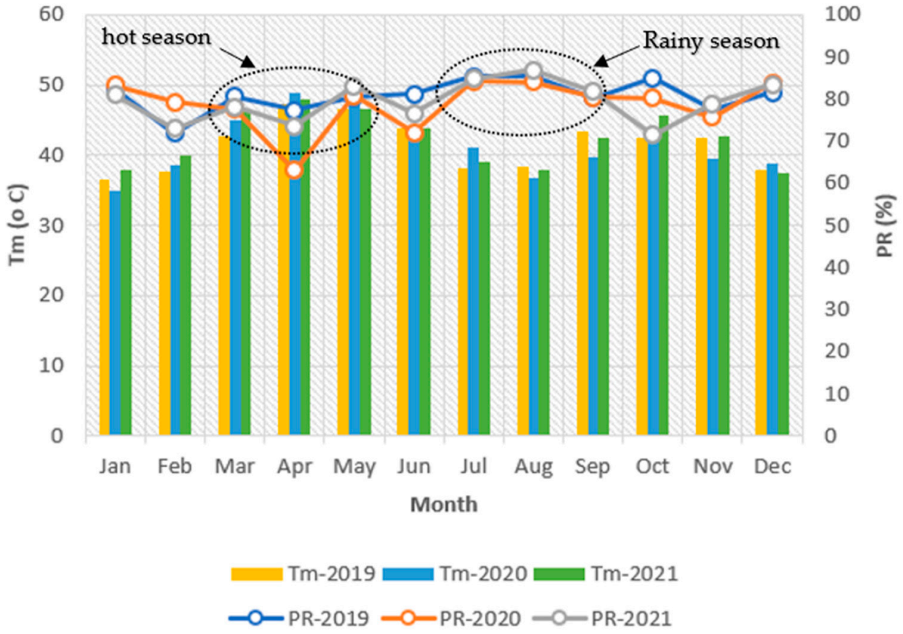

Figure 16. Monthly representation of module temperature (Tm) and performance ratio (PR).

Over the monitoring period, Figure 17 shows how the average daily final yield, capture, and system losses vary every month. The capture losses varied from 0.58 h/day in July to 1.734058 h/day in February of the year 2019 and from 0.63458 h/day in August to 2.37958 h/day in April of the year 2020. The system losses ranged from 0.09058 h/day in July and 0.14458 h/day in February during the year 2019 and from 0.09258 h/day in June to 0.137658 h/day in March for the year 2020. Because the modules are naturally cleaned during the rainy season (July and August), there are fewer losses during those months than during the summer, when there are more losses because of soiling, dust, and poor maintenance.

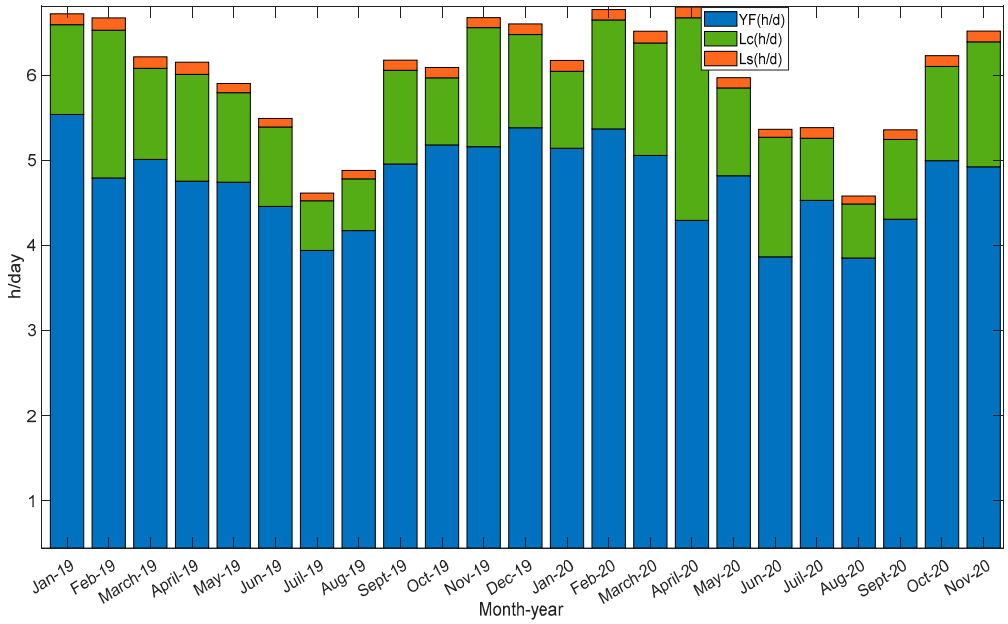

Figure 17. Monthly variation of final yield, capture losses, and system losses for the years 2019 and 2020.

Figure 18 depicts the evolution of the Zagtouli PV plant's capacity factor and solar irradiation. It can be seen that the capacity factor is globally proportional to the solar irradiation of the site; it is also closely related to the energy cost; and it demonstrates that the cost of PV electricity is very interesting in a high-sunset area like Zagtouli when compared to other less sunny areas. Furthermore, the annual capacity factor must be between 15% and 40% [38]. The Zagtouli plant has a capacity factor of 19.89% in 2019 and 19.29% in 2020.

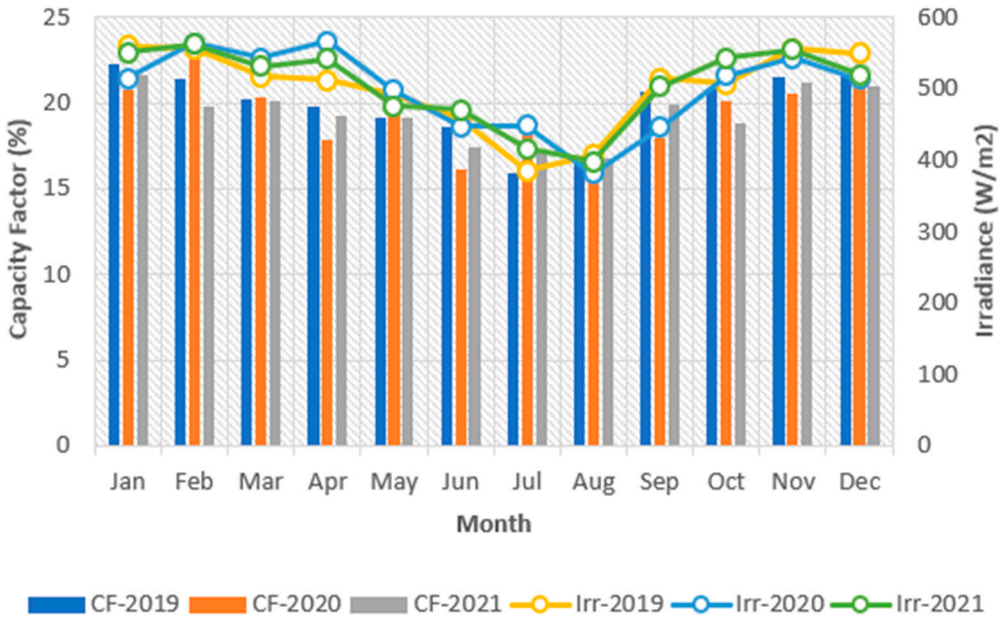

Figure 18. Monthly evolution of capacity factor with solar irradiation.

Table 5 below represents different yearly average yields, capture losses, array losses, and capacity factors for the years 2019, 2020, and 2021.

Table 5. Yearly yields, losses, and capacity factor.

Year	Yields (h/day)			Losses (h/day)		Capacity Factor (%)
	Y_R	Y_A	Y_F	L_C	L_S	
2019	6.08	4.96	4.84	1.05	0.12	19.91
2020	5.98	4.81	4.69	1.17	0.12	19.24
2021	6.06	4.92	4.79	1.14	0.13	19.33

Figure 19 shows the energy and exergy efficiencies, showing that the system's exergy efficiency is marginally higher than its energy efficiency over the entire study period, as confirmed by the second law of thermodynamics [35]. Since the modules are constantly cleaned and cooled, the ZGCPVS converts the maximum amount of solar energy received during the rainy season (June, July, and August). However, the hot and dusty seasons (March and April) are detrimental to the system's energy conversion, as confirmed by Wango et al. [39] and Kata et al. [40].

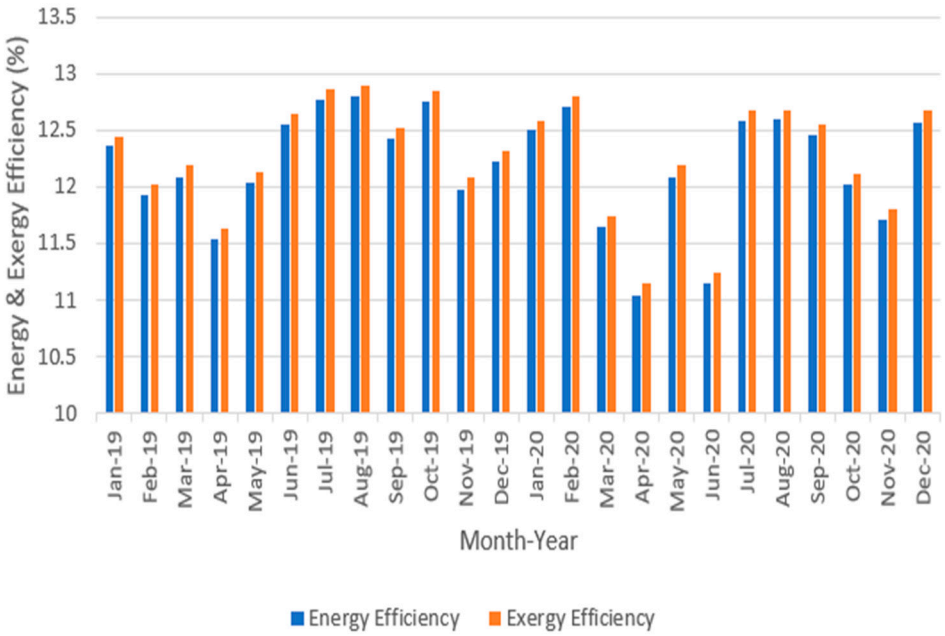

Figure 19. Monthly evolution of the PV System Energy and Exergy Efficiency.

Figure 20 represents the inverter efficiency with solar irradiation. To ensure profitability through the inverter, the irradiance must exceed 200 W/m^2. When the irradiation is above this value, there is a slight decrease in the performance of the inverter. Insufficient radiation below 200 W/m^2 adversely affects the performance of the inverter, leading to a decrease in the efficiency of the entire conversion chain. Consequently, this has a direct impact on the profitability of the solar power plant.

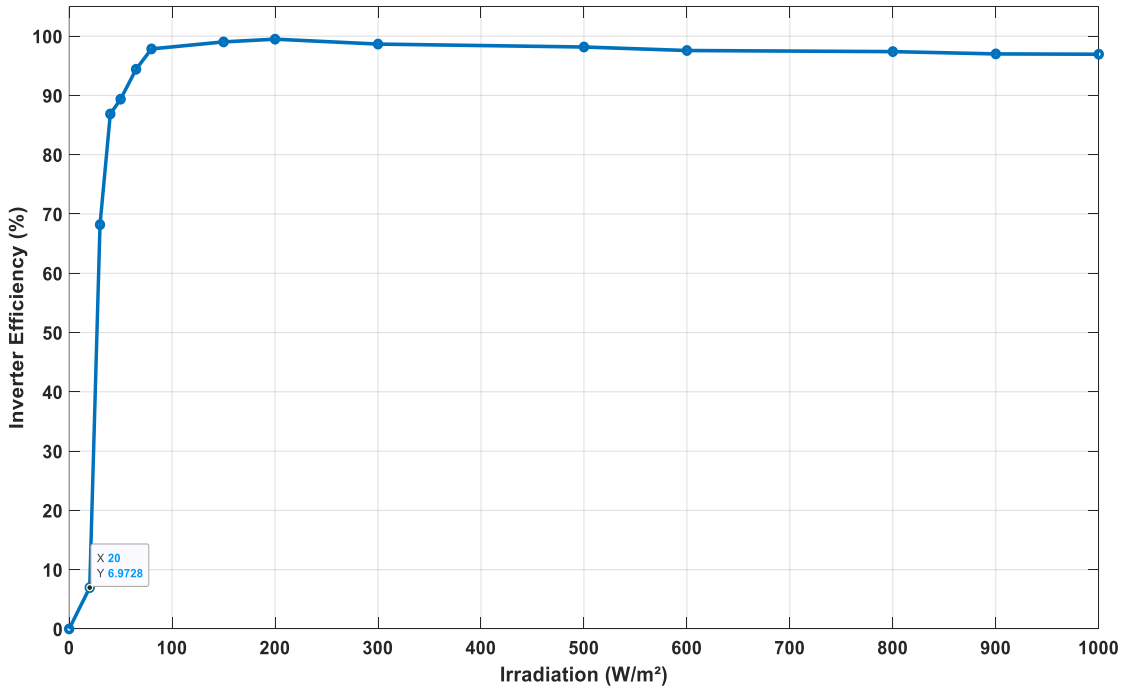

Figure 20. Inverter efficiency with irradiation.

Figure 21 shows the monthly evolution of the output energy of subsystem 2 using the PVGIS-SARAH2 database as well as the AC energy measured at the ZGCPVS site. The simulated and measured results are very close and follow the same trend. There is large

electricity production during the months of high solar irradiation. The energy output of the PV system varies over the three years of the study due to the constant change of seasons. A drop in production from June to August can be noticed because of cloud cover.

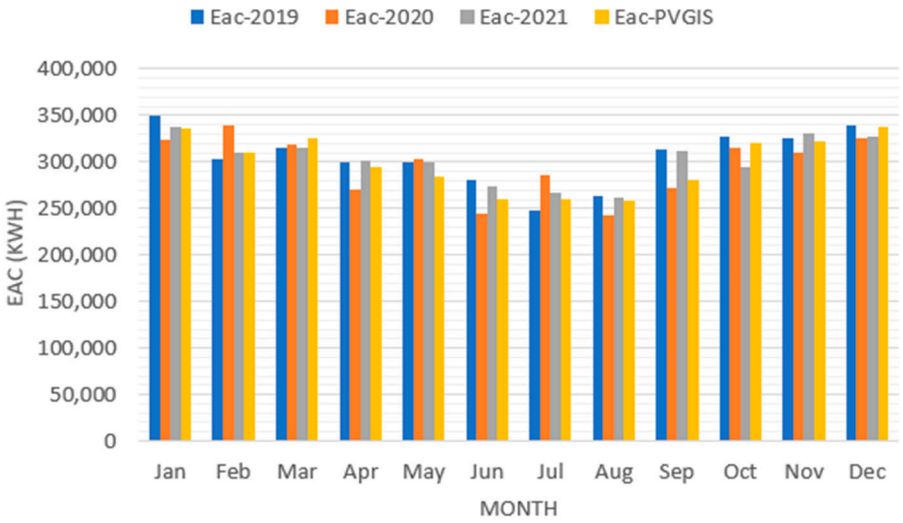

Figure 21. Monthly evolution of the total AC Energy injected by subsystem 2.

Table 6 below compares the performance of some PV systems around the world with that of Burkina Faso. For example, the PV system installed in Brazil has a lower final yield than the system installed in Burkina Faso but a higher performance ratio. The same is true for Ireland's PV system. The combined effect of high temperatures and dust reduces the PV system's performance ratio slightly in Burkina Faso despite the high solar energy resource (Figure 15). The system installed in Iran has the highest final yield and performance ratio. Because these values are comparable to those of the PV system in Burkina Faso, we can conclude that the ZGCPVS is performing satisfactorily.

Table 6. Comparison of ZGCPVS performance with other PV plants around the world.

PV System Location	Capacity (kWp)	Final Yield (h/d)	Performance Ratio (%)	Reference
India	10,000	4.20	78	[35]
Iran	5.52	5.38	82.92	[41]
India	5	3.99	76.97	[34]
Brazil	2.20	4.60	82.90	[7]
Mauritania	1500	4.28	73.56	[42]
Ireland	1.72	2.41	81.50	[32]
Spain	20	2.40	65	[43]
Lesotho	281	4.11	70	[44]
Burkina Faso (Actual)	33,000	4.89 (2019) 4.61 (2020) 4.92 (2021)	80.73 (2019) 78.70 (2020) 79.36 (2021)	

5. The Zagtouli Grid-Connected Solar PV System Socioeconomic Impacts

The initial step in providing electricity access to people is to increase the supply while reducing costs. This objective can be achieved through the development of solar energy production in Burkina Faso, a country with an estimated solar irradiation of 5.5 kWh/m^2/day. The construction of the ZGCPVS plant has played a significant role in expanding the available electricity supply and reducing the production cost per kilowatt-hour.

As an illustration, the ZGCPVS was projected to generate 55.529 GWh (gigawatt-hours) by 2020, accounting for approximately 9.7% of the SONABEL total electricity production [45]. This production from the PV plant has contributed to meeting the growing energy demand in the country. Furthermore, the estimated production cost for the Zagtouli

PV plant is $0.08 per kilowatt-hour, reflecting a lower cost compared to other traditional energy sources [46]. Moreover, the construction and operation of ZGCPVS have created job opportunities, both during the installation phase and in the ongoing maintenance and operation of the facility. This has contributed to employment generation and the development of local expertise in the renewable energy sector.

By harnessing solar energy and leveraging the capabilities of the ZGCPVS, Burkina Faso has made substantial progress in enhancing electricity supply and affordability. This development lays the foundation for expanding access to electricity and driving socio-economic growth in the country.

6. Conclusions

This study examined the performance of Burkina Faso's first and largest solar photovoltaic power plant. According to the findings, the temperature of the modules can reach 47 °C during the hot season. The system's overall daily yield is lower in the winter due to the constant inaccessibility of solar irradiation. Its daily average value in 2019 was 4.9 h/d, compared to 4.6 h/d in 2020 and 4.79 h/d in 2021. Thus, this PV plant performed better in 2019 than in 2020 and 2021. With an energy efficiency of 12.29% in 2019, 12.09% in 2020, and 12.10 in 2021, the performance ratio in 2019 was 80.73%, 78.70% in 2020, and 79.36% in 2021. The capacity factor was 19.89% in 2019, 19.29% in 2020, and 19.33% in 2021, which means that Solar PV production is cost-effective at the ZGCPVS site compared to other sites. The plant runs efficiently during the rainiest months (from July to September) and the coldest months (January, February, November, and December), but the hottest months (March and April) are extremely inconvenient for the activity of the ZGCPVS. This plant's final output comparison with other solar PV plants led to the conclusion that it is operating efficiently.

Future research on the ZGCPVS should focus on conducting a comprehensive analysis of its performance and proposing potential solutions. Several key areas warrant investigation:

1. Comparative analysis of sub-systems: A detailed comparison of the various sub-systems within the ZGCPVS will help identify specific weaknesses or inefficiencies. This analysis can assist in pinpointing areas that require improvement or optimization.
2. Analysis of plant disconnection from the SONABEL network: It is crucial to examine the plant's disconnection from the SONABEL network to optimize energy losses. Understanding the causes and effects of disconnection and developing strategies to minimize such occurrences will contribute to improving the plant's overall performance and reliability.
3. Economic assessment of a sophisticated cleaning mechanism: Evaluating the economic feasibility and benefits of implementing an advanced cleaning mechanism for the ZGCPVS is essential. This assessment should consider factors such as initial investment costs, operational expenses, energy production gains, and the overall profitability of the plant. A cost-benefit analysis will provide valuable insights into the potential advantages and drawbacks of adopting a more sophisticated cleaning approach.

By addressing these research areas, a more comprehensive understanding of the ZGCPVSs performance can be achieved. Furthermore, potential solutions and recommendations can be proposed to optimize the plant's efficiency, reliability, and economic viability.

Author Contributions: Conceptualization, S.F.P., S.W. and L.Y.; methodology, S.F.P. and L.Y.; software, S.F.P. and L.Y.; validation, S.W., T.N.N. and A.C.; formal analysis, S.F.P.; investigation, S.F.P., S.W. and L.Y.; resources, S.F.P. and L.Y.; data curation, S.F.P.; writing—original draft preparation, S.F.P. and L.Y.; writing—review and editing, S.F.P., T.N.N., A.C., S.W., K.R. and L.Y.; visualization, S.F.P. and L.Y.; supervision, S.W. and K.R. All authors have read and agreed to the published version of the manuscript.

Funding: This research was funded by Partnership for Skills in Applied Sciences, Engineering and Technology (PASET)-Regional Scholarship and Innovation Fund (RSIF).

Data Availability Statement: Not applicable.

Acknowledgments: This work is part of the ongoing PhD training supported by PASET-RSIF. We thank the Burkina Faso national electricity company (SONABEL) for their facilitation of the data collection at the Zagtouli PV Power plant site.

Conflicts of Interest: The authors declare no conflict of interest.

References

1. Osman, A.I.; Chen, L.; Yang, M.; Msigwa, G.; Farghali, M.; Fawzy, S.; Rooney, D.W.; Yap, P.-S. Cost, environmental impact, and resilience of renewable energy under a changing climate: A review. *Environ. Chem. Lett.* **2022**, *21*, 741–764. [CrossRef]
2. Rahbari, H.R.; Mandø, M. Energy Analysis of Molten-Salt Storage Integrated with Air-Based Brayton Cycle: Case Study of a Wind Farm in Denmark. In Proceedings of the 2023 8th International Conference on Technology and Energy Management (ICTEM), Babol, Iran, 8–9 February 2023. [CrossRef]
3. Task 1 Strategic PV Analysis and Outreach PVPS. Available online: https://www.iea-pvps.org/trends_reports/trends-2022/ (accessed on 2 November 2022).
4. Renewable Energy Agency. Renewable Energy Statistics 2021. Statistiques d'Énergie Renouvelable 2021. Estadísticas de Energía Renovable 2021. About IRENA. 2021. Available online: https://www.irena.org/publications/2021/Aug/Renewable-energy-statistics-2021 (accessed on 5 December 2022).
5. Moner-Girona, M.; Bódis, K.; Korgo, B.; Huld, T. *Mapping the Least-Cost Option for Rural Electrification in Burkina Faso: Scaling-Up Renewable Energies Performance—A Science Base on Photovoltaics Performance for Increased Market Transparency and Customer Confidence View Project*; Publications Office: Luxemburg, 2017. [CrossRef]
6. Attari, K.; Elyaakoubi, A.; Asselman, A. Performance analysis and investigation of a grid-connected photovoltaic installation in Morocco. *Energy Rep.* **2016**, *2*, 261–266. [CrossRef]
7. de Lima, L.C.; de Araújo Ferreira, L.; de Lima Morais, F.H.B. Performance analysis of a grid connected photovoltaic system in northeastern Brazil. *Energy Sustain. Dev.* **2017**, *37*, 79–85. [CrossRef]
8. Boddapati, V.; Nandikatti, A.S.R.; Daniel, S.A. Techno-economic performance assessment and the effect of power evacuation curtailment of a 50 MWp grid-interactive solar power park. *Energy Sustain. Dev.* **2021**, *62*, 16–28. [CrossRef]
9. Ouedraogo, A.; Diallo, A.; Goro, S.; Ilboudo, W.D.A.; Madougou, S.; Bathiebo, D.J.; Kam, S. Analysis of the solar power plant efficiency installed in the premises of a hospital—Case of the Pediatric Charles De Gaulle of Ouagadougou. *Sol. Energy* **2022**, *241*, 120–129. [CrossRef]
10. Schardt, J.; Heesen, H.T. Performance of roof-top PV systems in selected European countries from 2012 to 2019. *Sol. Energy* **2021**, *217*, 235–244. [CrossRef]
11. Mihov, V.; Gabrovska-Evstatieva, K.; Trifonov, D.; Mihailov, N. Performance Analysis of a Grid-Connected PV Park in Ruse, Bulgaria. In Proceedings of the 2022 8th International Conference on Energy Efficiency and Agricultural Engineering (EE&AE), Ruse, Bulgaria, 30 June–2 July 2022; pp. 1–5.
12. Bouacha, S.; Malek, A.; Benkraouda, O.; Arab, A.H.; Razagui, A.; Boulahchiche, S.; Semaoui, S. Performance analysis of the first photovoltaic grid-connected system in Algeria. *Energy Sustain. Dev.* **2020**, *57*, 1–11. [CrossRef]
13. Lindig, S.; Ascencio-Vasquez, J.; Leloux, J.; Moser, D.; Reinders, A. Performance Analysis and Degradation of a Large Fleet of PV Systems. *IEEE J. Photovolt.* **2021**, *11*, 1312–1318. [CrossRef]
14. Fuster-Palop, E.; Vargas-Salgado, C.; Ferri-Revert, J.C.; Payá, J. Performance analysis and modelling of a 50 MW grid-connected photovoltaic plant in Spain after 12 years of operation. *Renew. Sustain. Energy Rev.* **2022**, *170*, 112968. [CrossRef]
15. Malvoni, M.; Kumar, N.M.; Chopra, S.S.; Hatziargyriou, N. Performance and degradation assessment of large-scale grid-connected solar photovoltaic power plant in tropical semi-arid environment of India. *Sol. Energy* **2020**, *203*, 101–113. [CrossRef]
16. Kumar, B.S.; Sudhakar, K. Performance evaluation of 10 MW grid connected solar photovoltaic power plant in India. *Energy Rep.* **2015**, *1*, 184–192. [CrossRef]
17. Wittmer, B.; Mermoud, A.; Schott, T. Analysis of PV Grid Installations Performance, Comparing Measured Data to Simulation Results to Identify Problems in Operation and Monitoring. In Proceedings of the 30th European Photovoltaic Solar Energy Conference and Exhibition, Hamburg, Germany, 14–18 September 2015; pp. 2265–2270. [CrossRef]
18. Umar, N.H.; Bora, B.; Banerjee, C.; Umar, N.; Panwar, B.S. Comparison of different PV power simulation softwares: Case study on performance analysis of 1 MW grid-connected PV solar power plant. *Int. J. Eng. Sci. Invent.* **2018**, *7*, 11–24.
19. KhareSaxena, A.; Saxena, S.; Sudhakar, K. Energy performance and loss analysis of 100 kWp grid-connected rooftop solar photovoltaic system. *Build. Serv. Eng. Res. Technol.* **2021**, *42*, 485–500. [CrossRef]
20. Goel, S.; Sharma, R. Analysis of measured and simulated performance of a grid-connected PV system in eastern India. *Environ. Dev. Sustain.* **2021**, *23*, 451–476. [CrossRef]
21. Cubukcu, M.; Gumus, H. Performance analysis of a grid-connected photovoltaic plant in eastern Turkey. *Sustain. Energy Technol. Assess.* **2020**, *39*, 100724. [CrossRef]
22. Boulmrharj, S.; Bakhouya, M.; Khaidar, M. Performance evaluation of grid-connected silicon-based PV systems integrated into institutional buildings: An experimental and simulation comparative study. *Sustain. Energy Technol. Assess.* **2022**, *53*, 102632. [CrossRef]

23. Saleheen, M.Z.; Salema, A.A.; Islam, S.M.M.; Sarimuthu, C.R.; Hasan, Z. A target-oriented performance assessment and model development of a grid-connected solar PV (GCPV) system for a commercial building in Malaysia. *Renew. Energy* **2021**, *171*, 371–382. [CrossRef]
24. Suri, M.; Huld, T.; Cebecauer, T.; Dunlop, E.D. Geographic Aspects of Photovoltaics in Europe: Contribution of the PVGIS Website. *IEEE J. Sel. Top. Appl. Earth Obs. Remote Sens.* **2008**, *1*, 34–41. [CrossRef]
25. Ilse, K.; Micheli, L.; Figgis, B.W.; Lange, K.; Daßler, D.; Hanifi, H.; Wolfertstetter, F.; Naumann, V.; Hagendorf, C.; Gottschalg, R.; et al. Techno-Economic Assessment of Soiling Losses and Mitigation Strategies for Solar Power Generation. *Joule* **2019**, *3*, 2303–2321. [CrossRef]
26. Myyas, R.N.; Al-Dabbasa, M.; Tostado-Véliz, M.; Jurado, F. A novel solar panel cleaning mechanism to improve performance and harvesting rainwater. *Sol. Energy* **2022**, *237*, 19–28. [CrossRef]
27. The International Electrotechnical Commission (IEC). Photovoltaic System Performance Monitoring—Guidelines for Measurement, Data Exchange and Analysis. IEC 61724. 1998. Available online: https://cir.nii.ac.jp/crid/1571698600443732992.bib?lang=en (accessed on 26 February 2023).
28. Sundaram, S.; Babu, J.S.C. Performance evaluation and validation of 5MWp grid connected solar photovoltaic plant in South India. *Energy Convers. Manag.* **2015**, *100*, 429–439. [CrossRef]
29. Abdul-Ganiyu, S.; Quansah, D.A.; Ramde, E.W.; Seidu, R.; Adaramola, M.S. Investigation of Solar Photovoltaic-Thermal (PVT) and Solar Photovoltaic (PV) Performance: A Case Study in Ghana. *Energies* **2020**, *13*, 2701. [CrossRef]
30. Boddapati, V.; Daniel, S.A. Performance analysis and investigations of grid-connected Solar Power Park in Kurnool, South India. *Energy Sustain. Dev.* **2020**, *55*, 161–169. [CrossRef]
31. Banda, M.H.; Nyeinga, K.; Okello, D. Performance evaluation of 830 kWp grid-connected photovoltaic power plant at Kamuzu International Airport-Malawi. *Energy Sustain. Dev.* **2019**, *51*, 50–55. [CrossRef]
32. Ayompe, L.M.; Duffy, A.; McCormack, S.J.; Conlon, M. Measured performance of a 1.72kW rooftop grid connected photovoltaic system in Ireland. *Energy Convers. Manag.* **2011**, *52*, 816–825. [CrossRef]
33. Al-Rasheedi, M.; Gueymard, C.A.; Al-Khayat, M.; Ismail, A.; Lee, J.A.; Al-Duaj, H. Performance evaluation of a utility-scale dual-technology photovoltaic power plant at the Shagaya Renewable Energy Park in Kuwait. *Renew. Sustain. Energy Rev.* **2020**, *133*, 110139. [CrossRef]
34. Yadav, S.K.; Bajpai, U. Performance evaluation of a rooftop solar photovoltaic power plant in Northern India. *Energy Sustain. Dev.* **2018**, *43*, 130–138. [CrossRef]
35. Kumar, M.; Chandel, S.S.; Kumar, A. Performance analysis of a 10 MWp utility scale grid-connected canal-top photovoltaic power plant under Indian climatic conditions. *Energy* **2020**, *204*, 117903. [CrossRef]
36. Agai, F.; Caka, N.; Komoni, V.S. Design Optimization and Simulation of the Photovoltaic Systems on Buildings in Southeast Europe. 2011. Available online: https://www.researchgate.net/publication/258047113 (accessed on 15 October 2022).
37. Jamil, I.; Zhao, J.; Zhang, L.; Jamil, R.; Rafique, S.F. Evaluation of Energy Production and Energy Yield Assessment Based on Feasibility, Design, and Execution of 3 × 50 MW Grid-Connected Solar PV Pilot Project in Nooriabad. *Int. J. Photoenergy* **2017**, *2017*, 6429581. [CrossRef]
38. Kazem, H.A.; Khatib, T.; Sopian, K.; Elmenreich, W. Performance and feasibility assessment of a 1.4kW roof top grid-connected photovoltaic power system under desertic weather conditions. *Energy Build.* **2014**, *82*, 123–129. [CrossRef]
39. Waongo, M.; Koalaga, Z.; Zougmore, F. A guideline for sizing Photovoltaic panels across different climatic zones in Burkina Faso. *IOP Conf. Ser. Mater. Sci. Eng.* **2012**, *29*, 012014. [CrossRef]
40. Kata, N.; Soro, Y.M.; Diouf, D.; Darga, A.; Maiga, A.S. Temperature impact on dusty and cleaned photovoltaic module exposed in sub-Saharan outdoor conditions. *EPJ Photovolt.* **2018**, *9*, 8. [CrossRef]
41. Edalati, S.; Ameri, M.; Iranmanesh, M. Comparative performance investigation of mono- and poly-crystalline silicon photovoltaic modules for use in grid-connected photovoltaic systems in dry climates. *Appl. Energy* **2015**, *160*, 255–265. [CrossRef]
42. Sidi, C.E.B.E.; Ndiaye, M.L.; El Bah, M.; Mbodji, A.; Ndiaye, A.; Ndiaye, P.A. Performance analysis of the first large-scale (15 MWp) grid-connected photovoltaic plant in Mauritania. *Energy Convers. Manag.* **2016**, *119*, 411–421. [CrossRef]
43. Drif, M.; Pérez, P.; Aguilera, J.; Almonacid, G.; Gomez, P.; de la Casa, J.; Aguilar, J. Univer Project. A grid connected photovoltaic system of 200kWp at Jaén University. Overview and performance analysis. *Sol. Energy Mater. Sol. Cells* **2007**, *91*, 670–683. [CrossRef]
44. Mpholo, M.; Nchaba, T.; Monese, M. Yield and performance analysis of the first grid-connected solar farm at Moshoeshoe I International Airport, Lesotho. *Renew. Energy* **2015**, *81*, 845–852. [CrossRef]
45. SONABEL. Rapport D'activités 2020. 2020. Available online: https://www.sonabel.bf/a-propos/documentation/ (accessed on 1 July 2023).
46. Alliance Sahel. Available online: https://www.alliance-sahel.org/actualites/centrale-solaire-de-zagtouli/ (accessed on 2 July 2023).